Preparation of MgO Nanoparticles by Pulse Laser Ablation in Liquid for Biological Applications

Doaa Omar Chyad Khalil

University of Baghdad/ College of Science for Women Medical Physics Department/ Do620174@gmail.com

ABSTRACT

Mg nanoparticles were prepared by PLAL method by placing the element in ionic water with a depth of 3ml and bombarded with a Nd-YAG laser with a wavelength of 1064nm and the number of pulses 100 pulses for each energy (300, 400 and 500) at a fixed frequency of 6hzThe concentration of the elements was calculated by atomic absorption spectrometry (AAS) and the result was (17.4, 27.4, 19.4), respectively. The values of the optical energy gap, which is one of the most important optical constants in semiconductor physics, were calculated by analyzing the UV absorbance spectrum with three concentrations (17.4, 27.4, 19.4), and it was noticed that the higher the concentrations, the lower the energy gap. The particle size was determined by X-ray diffraction (xrd) technique and the crystal size increase of Mgo NPs was observed with increasing laser power by three (111) (220) (331) peaks .The shape of the nanoparticles was known by taking FE-SEM images with a magnification capacity of 330 kx with (300,400,500) mJ, and it shows that they are cube-shaped with different diameters for each sample grouped together with an average size of (100,200,300) respectively of energies (300,400,500) for MgO Nps. The effect of Mgo NPs in the process of inhibiting it was tested against two types of negative bacteria(E. Coli and pseuedomonas aeruginosa) and two types of positive bacteria (s. aurous and streptococcus pyogenes)The sample showed 400 mJ activity against one type of chromosomal bacteria, which is streptococcus pyogenes, with a measure of 22 mm, and a high activity against E. coli (22 mm, 25 mm, 32 mm). And pseudomonas aeruginosa (20mm,28mm,32mm)

Keywords: Pulse Laser, Biological Nanoparticles

Introduction

Plasma, is a quasi-neutral gas, it is the fourth state of matter which exhibits collective behavior, it represented 99% of the matter in the universe, but not all plasmas are identical. It has a variety of different temperatures and densities, and we can say that we live in the 1 % of the universe which does not have plasma naturally. States of matter Plasma consists of a mixture of reactive components [2] including charged species (positive and negative ions, electrons , neutrals, reactive oxygen and nitrogen species ROS and RNS, and other components as shown in Figure (1.2).

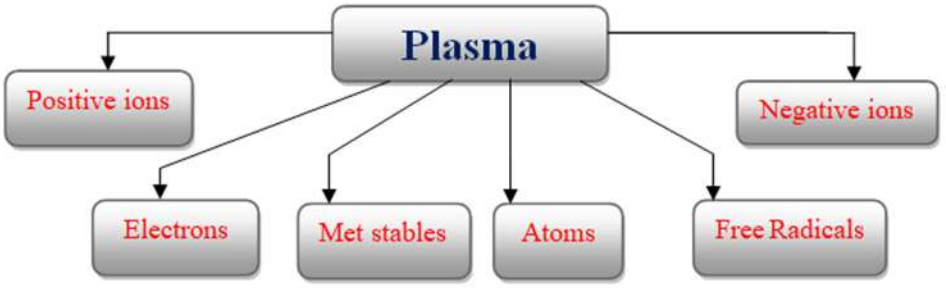

Figure (1.2) :Constituents of plasma [3].

1-2 Nanoparticles

Although the word (nanoparticles) is modern in use, these particles have been present in manufactured or natural materials since ancient times. For example, some beautiful colors appear from rusted glass windows because of the presence of very small clusters of metal oxides in Glass has a size close to the wavelength of light. Hence, particles of different sizes scatter different wavelengths of light, resulting in different colors of glass appearing [4]. Nanoparticles can be defined as a microscopic atomic or molecular assembly ranging from a few atoms (molecule) to a million atoms, bound together almost spherically with a radius of less than 100 nanometers, a particle with a radius of one nanometer will contain 25 atoms, most of which are on the surface The particle, and this differs from the molecule, which may include a number of atoms, that the dimensions of the nanoparticle are less than critical dimensions necessary for the occurrence of certain physical phenomena, such as: the average free path traveled by electrons between two successive collisions with vibrating atoms, and this occurs with electrical conductivity [5]

Atomic assembly has magic numbers of atoms to form nanoparticles. Silicon nanoparticles, for example, consist of specific numbers of atoms and not at any number, to create particles with specific radii of only 1,1.67,2.15,2.9 nanometers. When these particles are exposed to ultraviolet rays If it is violet, it emits light of a visible color whose wavelength is inversely proportional to the square of the particle's diameter, so certain visible colors can be seen.

When the size of nanoparticles reaches the nanoscale in one dimension, it is called a quantum well, but when its nanoparticle size is in two dimensions, it is called the quantum wire, and when these nano-sized particles are in three dimensions, they are known as quantum dots), and it must be pointed out here that the difference in the nanoscale dimensions in the three aforementioned structures will affect their electronic properties, causing a significant change in the optical properties of the nanostructures [6].

1-3 Nanomaterials properties

One of the important and unexpected properties of nanoparticles is that the surface properties of the particles overcome the volumetric properties of the material, while the physical properties of the volumetric material are constant regardless of its size. Semiconducting nanoparticles, surface plasmon resonance in some metal nanoparticles. It is also noted that the percentage of surface atoms of the material becomes very important when the size of the material approaches the nanoscale, while when the volumetric material is greater than 1 micrometer, the percentage of atoms at its surface will be very small in relation to the total number of atoms in the material. Another characteristic of nanoparticles is that they can be attached to a liquid or solution without floating or submerging; This is because the interaction between the surface of the particles and

the liquid is so strong that it overcomes the density difference between them, which is usually responsible for the buoyancy or immersion of the volumetric substance in the liquid [7].

It has recently been possible to manufacture nanoparticles of metals, insulators, semiconductors and hybrid structures (such as coated nanoparticles), in addition to manufacturing models of nanoparticles of a semi-solid nature, namely liposomes, and other forms of nanoparticles are semiconducting quantum dots and nanocrystals. Copper nanoparticles with a size of less than 50 nanometers are considered to be of high hardness and are not malleable or ductile, unlike what happens to ordinary copper, as they can be easily bent, knocked and pulled [8].

Nanoparticles can be natural particles that are already present in nature, such as nanoclay nanoparticles and cellules nanofibers, as well as silicon particles and its compounds such as nanosilicon carbide, and in most cases these particles are processed to become suitable for practical tests and industrial applications. It is also possible to obtain industrial nanoparticles, such as nanogold nanoparticles, nanosilver, carbon nanotubes, and others. These industrial particles can be prepared in two ways: [9]:

1. Bottom-up method

2. Top-down method

1. Bottom-up method

Bottom-up methods involve assembling atoms or molecules into nanostructured arrays. In these methods the sources of raw materials can be in the form of gases, liquids or solids. The latter requires some kind of disassembly before incorporating them into a nanostructure. Bottom-up methods generally fall into two categories: chaos and control . Chaotic processes involve raising the constituent atoms or molecules into a chaotic state and then suddenly changing conditions to make that state unstable. By clever manipulation of any number of parameters, products are shaped largely as a result of insurance kinetics. It can be difficult or impossible to control the breakdown caused by chaos, so aggregate statistics often govern the resulting size distribution and average size. Accordingly, the formation of nanoparticles is controlled by manipulating the final state of the products. Examples of chaotic processes include laser ablation, [10] blast wire, arc, flame pyrolysis, combustion, and deposition synthesis techniques. Controlled processes involve the controlled delivery of constituent atoms or molecules to the nanoparticle formation site(s) so that the nanoparticles can grow to specific sizes in a controlled manner. In general, the state of the constituent atoms or molecules is never far from that required for the formation of nanoparticles. Accordingly, the formation of nanoparticles is controlled by controlling the state of the reactants. Examples of controlled processes are self-limiting growth solution, self-limited chemical vapor deposition, femtosecond-pulse laser techniques, and molecular beam amplification.

2. Top-down method

Top-down methods take some "force" (such as mechanical force and lasers) to break up bulk materials into nanoparticles. A common method that involves mechanical disintegration of bulk materials into nanomaterials is "ball milling". Besides, nanoparticles can also be made by laser ablation which uses a short-pulsed laser (such as a femtosecond laser) to excise a target (solid) [11].

1-4 Magnesium

In recent years, many researchers have noted to mag- nesium microstructures and nanostructures due to their novel properties to distinguish them from bulk materials and diverse applications in fields of propellant, battery, composite fillers, etc. Magnesium has several very promis- ing properties for applications in plasmonics and specially in switchable plasmonic metamaterials [12]. As reported by Sterl et al, magnesium nanoparticles exhibit a pronounced plasmonic response at throughout the whole visible wave- length range. Therefore, it can be an ideal alternative to established materials for UV plasmonics such as aluminum [13]. Magnesium is an excellent candidate for weight critical structural applications for its impressive low mass density. A good high temperature crawl, a high damping capacity. And good dimensional stability are the properties that make magnesium perfect for industrial applications [14]. Magnesium is a candikdate for the fuel cell technologies. It is re- versible, abundant and low-cost element possesses the large capacity for hydrogen storage (7.6 wt%) [15].

1-5 Laser Ablation

It is a technique used to remove materials from a solid surface that includes the energy of the absorbed laser and evaporates mainly when material is heated when the laser is flowing and the material is converted to the plasma in the case of high flow.

Laser ablation is one of the most efficient physical methods for nono fabrication. The method consists in the ablation of a target (mostly solid) by an intense laser radiation, yielding to an ejection of its constituents and to the formation of nanoclusters and nanostructures. When the target is ablated in vacuum or in a residual gas, the nanoclusters can be deposited on a substrate, placed at some distance from the target, leading to the formation of a nanostructures film [14].

1.6 Pulsed Laser Ablation in Liquid (PLAL)

Laser ablation in liquid demonstrates as alternative way to create nanoparticles useful in a wide range of applications. PLAL has been used to prepare various kinds of nanoparticles such as metals, oxides, alloys, and semiconductors [12]. As shown in figure (2.3).

Figure (1.3):- demonstrates the setup of PLAL technique

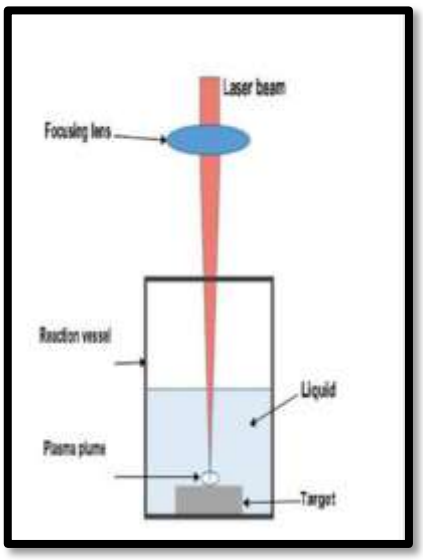

PLAL has many desirable advantages. It is a simple one-step process and effective technique for preparing nanoparticles in large quantities suspended in liquid [13]. The ablation process is takes place in an environment that does not require high pressure or high temperature. PLAL production system is a low cost and has contains chemically simple materials that do not need a catalyst. These factors ensure the production of extremely small and clean nanoparticles that can have high surface activity [14]. PLAL produces a wide range of nanoparticles formation, which is difficult to obtain in usual methods. Finally, it presents an efficient approach to control the nanoparticles size and morphology by varying the laser physical parameters such as laser energy, wavelength, repetition rate, focusing condition, pulse duration and number of pulses or liquid parameters such as temperature, type, PH level and surfactant [11].

The PLAL process mainly depends on the removal of target immersed in the liquid by laser pulses that stimulate the plasma. This plasma is a product of the ionization absorption and laser photons in the gas phase resulting from the ablation process. It is directly related to the laser pulse and influenced by the properties of incoming pulse, such as the lighting, pulse duration, wavelength. The plasma column consists mainly of neutral ions and atoms, and the electrons evaporate from the target and its expansion is limited to the liquid medium in which it occurs [15].

The solid target continues to absorb laser radiation, which creates more evaporating types, which widens the shaft, creating a shock wave with a high temperature and pressure. This is called plasma induced pressure and helps increase the temperature, density, and pressure of the laser –induce plasma [15].

A thin layer of vapor with high temperature is created due to energy transfer from plasma to the surrounding liquid during the plume expansion and condensation, creating cavitational bubbles. The vapor expands and transforms into bubbles with a radius larger than the vapor layer. The pressure inside the bubbles is increased by liquid confinement [14].

The plasma column cools down after its energy is transferred to the vapor layer. This leads to the expansion of bubbles in each direction of bubbles in each direction that moves against the liquid and the compressed plasma, then gradually balances the internal pressure bubbles with the surrounding liquid and reaches the maximum radius. Bubbles maintain this condition for some time. Finally, it breaks down and releases nanoparticles into the liquid. Nanoparticles are produced during plasma contraction. They arise from the interaction of liquid and target molecules. After that, it spreads into the twisting bubbles and is finally released to the solution [13]. Figure (1.4) illustrates the time sequence for the PLAL process.

Figure (1.4): Mechanism of PLAL and time sequence [13]

At the liquid and plasma induced by laser interface, there are four chemical reactions happening during plasma transformation [14, 15, 16]:

1. A chemical reaction occurs within the laser-induced plasma between the ovarian types of target and the fixed stages resulting from the temperature, pressure and density of the plasma column.

2. A chemical reaction occurs also inside the laser-induced plasma but the reaction takes place between the ablated species of the target and excited liquid molecules.

3. A chemical reaction is induced due to high temperature, density, and pressure in the laser-induced plasma, which provides a good opportunity. Chemical reactions to high temperatures between liquid and laser-induced molecules.

4. A chemical reaction takes place between the ablated target species and liquid molecules inside the liquid. It produces nanoparticles suspended in the liquid which are made from atoms of both the target and the liquid medium.

Therefore, ablating a solid target immersed in a liquid by pulsed laser ablation has gained the researchers attention due to the possibility producing extreme conditions easily, which in turns leads to form new nanoparticles by easily changing the liquid medium and solid target [16].

1.7 Basics of Plasma

1.7.1 Debye Length

Debye length is the usual space-size characterizing plasma, which is a linear measure of shielding the external electric fields and electro neutrality. The essential property of plasma is the ability to shield out electric potential that applied it. If a cloud of electrons attracted

around the positive ion in plasma due to coulomb law. The closest electrons to the ion form a shield for the other electrons; in the same way the force between the shielded electrons and the ions is smaller than the Coulomb force without the shielding . That's why the attraction force of a cation is a finite distance, This distance is called Debye shielding as shown in Figure (1.5).

The Debye length λ_D is a function of temperature and density, it is a distance of shielding [2],

$$\lambda_D = \frac{\varepsilon^0 K T_e}{(e^2)}^{1/2} \quad \ldots\ldots(1.1)$$

$$\lambda_D = 69 \left(\frac{T_e}{2}\right)^{1/2} \quad \ldots\ldots\ldots(1.2) \qquad \text{T in K}$$

$$\lambda_D = 7430 \left(\frac{KT_e}{n}\right)^{1/2} \qquad \text{T in eV}$$

for a high temperature the Debye length becomes larger and for denser plasma becomes smaller. On the other hand, during a high temperature, the motion is larger and the efficiency of shielding decreased causing the Debye length to be increased. A gas can be considered as a plasma if the density of electrons high enough that the Debye length is smaller than the dimension of the plasma system [17].

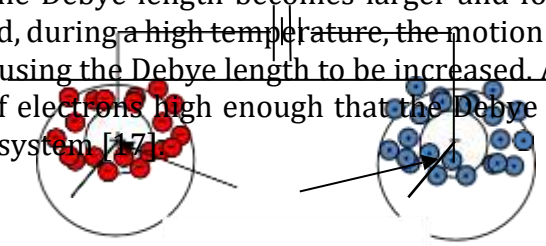

Plasma

λ_D

Debye shielding

1.7.2 Plasma Oscillation (Plasma Frequency)

The frequency of plasma is the typical plasma time scale and typical time of plasma response to the external fields. It is the reverse time that plasma needed to re-electroneutrality, the electron frequency is the most important character in plasma, due to electrons lighter than heavy ions, so, the mobility is higher than ion. The frequencies of residual particles that constituent plasma can be measured in a similar way.

The period that plasma needed to re-electroneutrality depended on the density $n_e \approx n_i \approx n$; it decreased when density increased, so, plasma frequency increased with density.

$$\omega_p = \left(\frac{ne^2}{\varepsilon_0 m}\right)^{1/2} \quad \ldots\ldots\ldots (1.3)$$

So, the plasma frequency depends only on plasma density as shown in Figure (1.4) and can be calculated as [18]:

$$\omega(s^{-1}) = 5.65 \times 10^4 \sqrt{n(cm^{-3})} \quad \ldots\ldots\ldots (1.4)$$

1.7.3 Temperature of Plasma

The temperature of plasma is defined by the average energies of plasma constituents (natural or charged) and degree of freedom that relevant (translational, rotational, vibrational and those related to excitation of electrons). As plasma have different species, it is display multiple temperature, described by the temperatures of each particle, including the temperature of electron T_e, temperature of ion T_i, temperature of gas T_g and temperature of neutral particles T_0.

In all plasma that is generated by electric field, electrons are lighter than heavy ions, so, it receives the external energy from electric field, during collision with heavy particles (Joule heating) much faster than the heavier ions and have a set of circumstances to heat up to several thousands of degrees before their environment

heats up, for this reason electrons have a higher temperature than ions[19]. According to the Maxwell-Boltzmann distribution, the average kinetic energy of a particle can be written as in (1.5):

$$E = \frac{3}{2} K_B T \dots\dots\dots (1.5)$$

Generally, for ionizing molecules, the energy required is greater than ~10 eV. It is very common to express temperature in an energy unit of eV by using K_BT , eV= K_BT. Low temperature plasmas are typically categorized into two major groups: when the temperature affected depended essentially on treatment, it is called thermal plasma, and when the constituent of plasma (positive and negative ions, electrons, radical, ultraviolet radiation) are used is called a non thermal plasma, it is summarized in table (1.1) [3].

Table (1.1): Classification of plasma [3].

Plasma	**High-temperature plasma (Equilibrium plasma)**	**Low temperature plasma**	
		Thermal plasma (Quasi-equilibrium plasma)	Non thermal plasma (Non-equilibrium plasma)
State	$T_e \approx T_i \approx T_g = 10^6\text{-}10^8$K $n_e \geq 10^{20}$ m^{-3}	$T_e \approx T_i \approx T_g \leq 2\times10^4$ K $n_e \geq 10^{20}$ m^{-3}	$T_e >> T_i \approx T_g = 300\text{-}10^3$K $n_e \approx 10^{10}$ m^{-3}
Example	Laser fusion plasmas	Arc plasma, plasma torches	Glow, corona, APPJ, DBD, plasma needle

1.7.3.1 Thermal Plasma

In a thermal plasma, energy flux from electrons to heavy ions equilibrates to the energy flux from heavy ions to the environment only when temperatures of ions and electrons become equilibrium

$T_e \approx T_i \approx T_g \leq 2\times10^4$ K. So that, thermal plasma is called quasi- equilibrium plasma which is in a local thermal equilibrium (LTE).

To produce thermal plasma, different devices like Arc plasma, plasma torch, and microwave devices can be used. These sources are mainly used in areas such as plasma material processing and plasma treatment of waste materials [20].

Thermal plasma can be used in many different applications, such as preserving the environment by using plasma to treat industrial wastes (plasma gasification) [18], and reducing environmental pollution by

destroying toxic substances [19], chemical vapor deposition [20], thermal plasma using in surgery for coagulation and tissue cutting. So, thermal plasma may be considered undesirable in some cases due to high temperature. Moreover, high-coasted manufactured and maintenance of thermal and power plasma systems [21].

1.7.3.2 Non-thermal plasma

Non thermal plasma is generated by a high voltage causing electrical discharge, despite of high temperature of electrons approximately 10 eV; it is called a non thermal because the mass of ions is much larger than the mass of electrons and because of its small mass, it acquires a thousand times of energy higher than heavy ions to reach high temperature before the surrounding ions, temperature of cold plasma devices normally operate below 40°C, $T_e >> T_i \sim T_g \sim 300$ K [17]. Therefore, this property can be used in cases that are sensitive to high temperatures such as a living tissue and some biological applications, it is effective and safety for medical applications that have individual requirements, whose inhibits tissues to heating in some applications. Such as operation at low temperature and open atmospheres [3], painless in vivo applications and without damaging the surrounding tissue [22] .

1.8 Criteria for Plasma

There are three conditions that must satisfy in an ionized gas to be called plasma [2]:

1- Debye length $\lambda_D << L$ it is the required condition to satisfy collective behavior for plasma, it is satisfied when the dimension of system (L) is much larger than the Debye length (λ_D), consequently, in semiconductor the system decreased when the density increased, which causes reducing in the Debye length (λ_D); this method is used in Diodes circuits.

2- number of charged particles in Debye sphere $N_D >>> 1$, collective behavior required a huge number of charged particles (N_D) in Debye sphere.

$$N_D = n\frac{4}{3}\pi\lambda_D^3$$

$$N_D = 1.38 \times 10^6 T^{3/2}/n^{1/2} \qquad (T \text{ in } K^o) \ldots\ldots\ldots (1.7)$$

3- plasma frequency $\omega_p\tau > 1$this condition is related to collisions,

ω_p is the plasma frequency and τ is the mean time between collisions with neutral particles; this means that the time of collisions must be more than required time that needed to re- electroneutrality, in another meaning plasma frequency must greater than the collision frequency of charged particles.

1.9 Optical Properties of Nanoparticles

The optical band gap was estimated graphically by applying Tauc's relation for direct transition [23].

$$(\alpha h\nu) = (h\nu - E_g)^r \cdots\cdots\cdots\cdots\cdots\cdots\cdots\cdots\cdots\cdots (1\text{-}8)$$

Where A is constant, h is plank's constant, υ is the incident photon frequency, is optical energy gap and r is a constant depending on the

nature of transition. r value representing the optical transmission mode; when r = 1/2 the transition mode is direct allowed, r = 3/2 direct forbidden, r = 2 indirect allowed, and r =3 indirect forbidden. The optical energy gap was determined by plotting versus the photo energy and extrapolating the linear portion of $(\alpha h\vartheta)^2$ and

($3/_2$, the value gives the optical energy gap for direct $\alpha h\vartheta$)

transitions.

1.10 Bacteria:

1. 10.1. Escherichia coli

It is a Gram-negative bacilli, coexisting in the intestinal tract of humans and animals.

It has an optimal growth temperature of 37 degrees Celsius, but it can grow in wide thermal ranges between (45-15) degrees Celsius

And it affects the soft tissues, so it is considered an opportunistic bacteria that causes gastrointestinal infections, wounds, sepsis, and urinary tract infections

1.10.2. Pseudomonas aeruginosa

These bacteria are found in soil, water, plants, skin, and most environments, whether natural or man-made.

It has multiple possibilities. When it infects an organism, it destroys its tissues and infects organisms that suffer from immunodeficiency. Symptoms of her diseases are inflammation and sepsis. If it spreads to vital body systems, such as the lungs, urinary tract, or kidneys, it can be fatal

1.10.3.Streptococcus pyogenes

Positive bacteria

It has an important role in human diseases. Infection rarely what happens, but it is usually a nurse

It can lead to diseases, which often produce small areas of beta -type blood decomposition, and a comprehensive destruction of all red blood cells

2.1 Introduction

This chapter covers the experimental part and the techniques used during this project. It consists of two parts. ***Part One***: Synthesis of Nanoparticles by physical methods (Pulse Laser Ablation in Liquid PLAL) for element (MgO). ***Part Two:*** it includes the biological part, which is the effect of Nanoparticles manufactured by physical methods on the bacterial inhibition of the two types of Gram-positive and Gram-negative bacteria. Figure 2-1 shows a schematic diagram of the experimental work**.**

Work layout

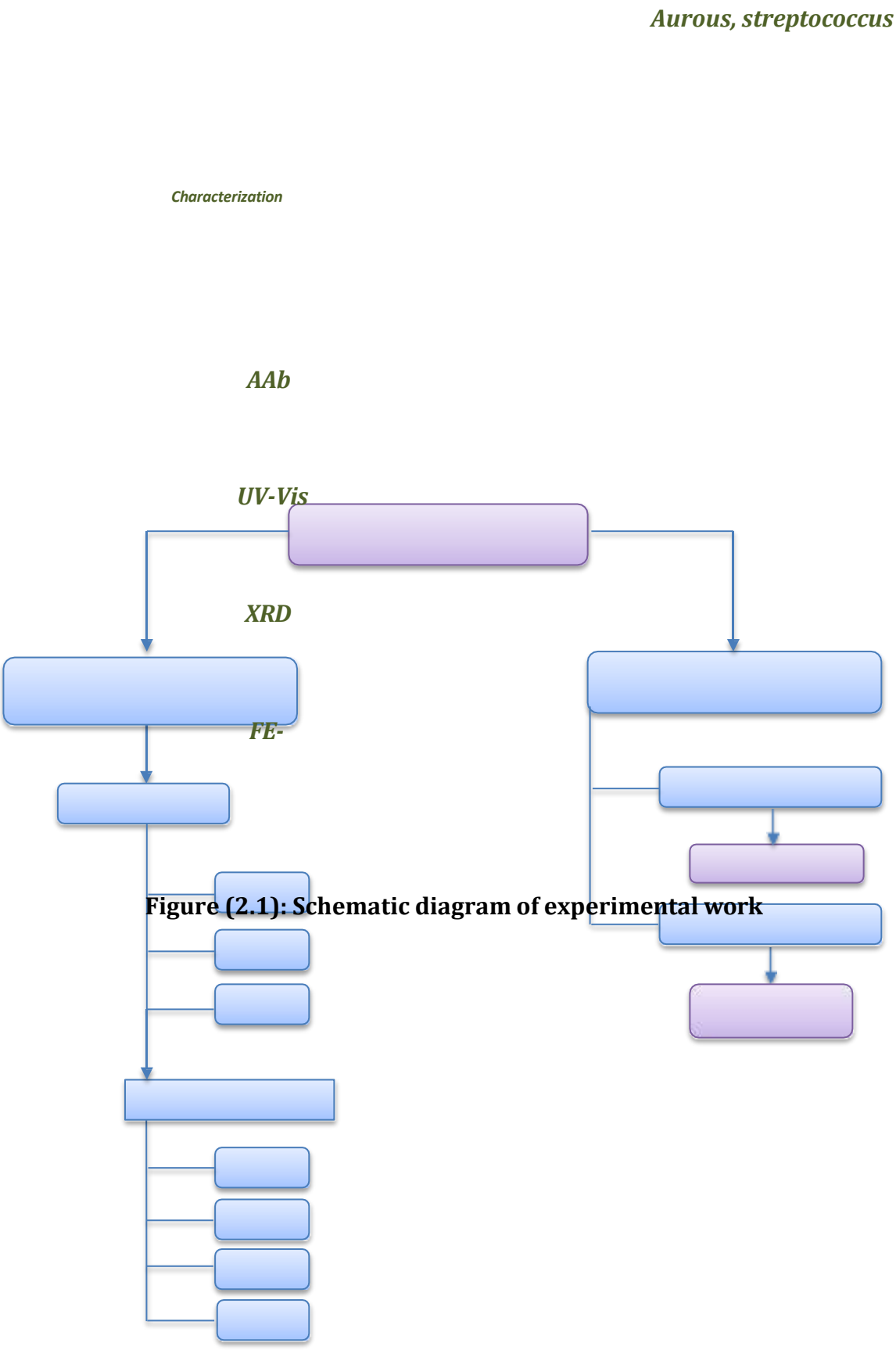

Figure (2.1): Schematic diagram of experimental work

2.2 Laser System

Laser parameters are listed in Table (3.1). The laser beam was focused by a convex lens with a focal length of 100 mm. After focusing, the laser beam spot size was measured using optical inspection peak scale loupe magnification microscope (part No. TS- 1983, START International, USA) and found to be 2.2 mm. The laser energy was calibrated using Gentec-CO joule meter (model: MAESTRO, A pulsed Q-switch Nd:YAG laser (Model HF -301, Huafei technology, China) that is shown in Figure (3.3) was employed as a pulsed laser ablating source. The Gentec Electro-Optic, Quebec City, Canada).

The laser is going out through the gun hand piece and was mentioned earlier. We must be aware that the number of pulses in device in from 0-999999 and then it is necessary to reset the laser in order to prepare it for working again (reset pulse counter). It should be noted here that it is almost efficiency and cleanliness of water. It is worth mentioning that the operating temperature must not exceed 37℃ in order to keep the machine out of damage and malfunction of internal active medium YAG crystal.

Figure (2.2): Q-switched Nd:YAG laser

Table (2.1): laser parameters

Energy	**20- 2000 mJ/pulse**
Pulse duration	**10 ns**
Wavelength	**1064 nm**
Spot size	**2.2 mm**
Frequency	**1-10 Hz**

2.3 Laser Focusing

Nd: YAG laser focusing on the target surface has been done using a convex spherical quartz lens with focal length 10cm and the lens has been placed inside the vacuum chamber. This laser focusing is necessary in order to exceed the ablation threshold energy density when the laser hit the surface of target material.In this experiment, the laser beam is manually coordinated with the target plane .The calibration and alignment have been optimized through the use of a visible laser beam considered as a guide to Nd: YAG laser because it is seen as a visible red color.

Changing the lens to a few millimeters of surface distance will affect the analyte strength. Hence it is very important for device accuracy and precision to keep the distance set during the measurements. We've used a 10 focal length lens in this work. A shorter focal lens can produce a small beam waist and thus a stronger breakdown but it also has a limited focus range.

2.4 Synthesis nanoparticles

2.4.1 Pulsed Laser Ablation in Liquid Technique PLAL

Figure (2.3) shows the experimental setup of PLAL based on the pulsed laser ablation in liquid environment method. Nanoparticles were synthesized by pulsed laser ablation of Ag target placed at the bottom of a glass vessel containing 3 ml of ionic water. Ionic water height above the target was 10mm. The target was irradiated by

Nd:YAG laser fluencies for 300, 400 and 500 mJ for 100 pulses. During the laser, irradiation process the vessel was rotated so that the nanoparticles formed did not shield the laser radiation from reaching the target surface. After the ablation process, the transparent becomes the ionic water colored in gray when irradiating for the MgO target, which gives the expectation of NPs formation. In PLA, laser parameters such as influence, wavelength, and pulse duration can monitor the size of Nano clusters [104].

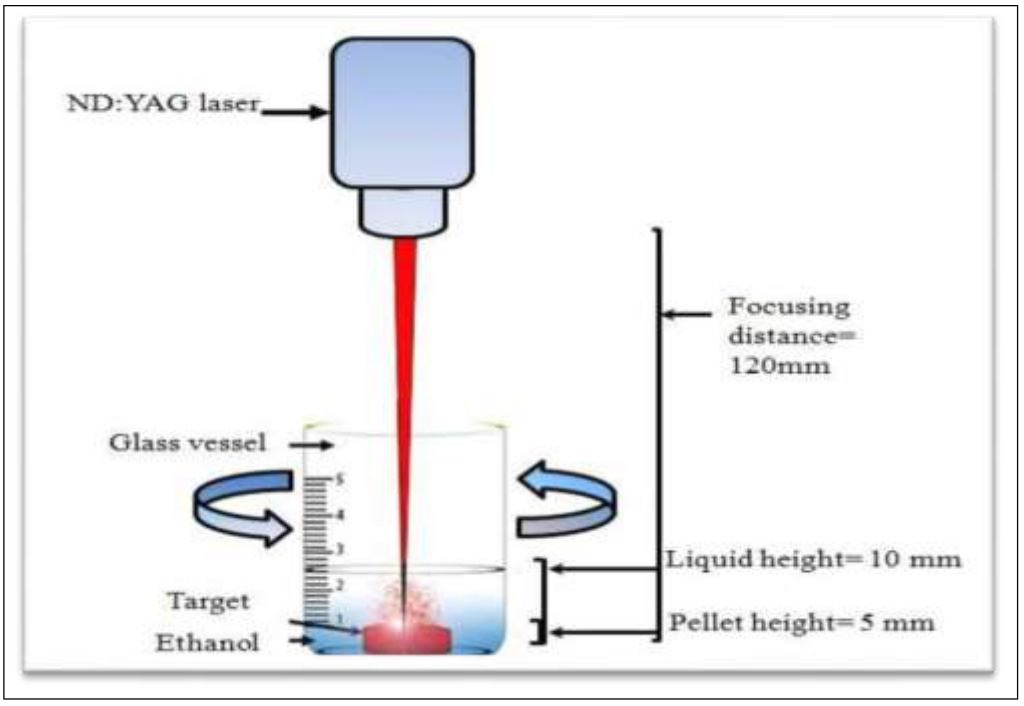

Figure (2.3): Experimental setup Laser ablation in liquid of synthesizes of MgO NPs.

2.5 Thin films preparation

Pure of (MgO) films under were prepared vacuum (P = 2.5 × 10^{-2} mbar) and optical and structural properties have been studies. The aim of this study is to determine the crystal structure through measurements (XRD and FE-SEM) of (MgO) films at first harmonic of Nd: YAG laser.

(MgO) thin film has been synthesized by drop coasting method under room temperature and on the microscope glass substrates (1× 25 × 75m).

2.6 The Measurement Techniques

2.6.1 Atomic absorption spectrometry

Atomic absorption spectrometry (AAS) is an analytical method used to calculate the element concentrations. Atomic absorption is accurate in a sample, it is capable of measuring up to parts per billion of a gram (µgdm^{-3}). The technique uses wavelengths of light that are absorbed directly by an entity. It correspond to the energies that necessary to promote electrons at a higher energy level from one energy level to another. The spectrometry of atomic absorption has many applications in various areas of chemistry.

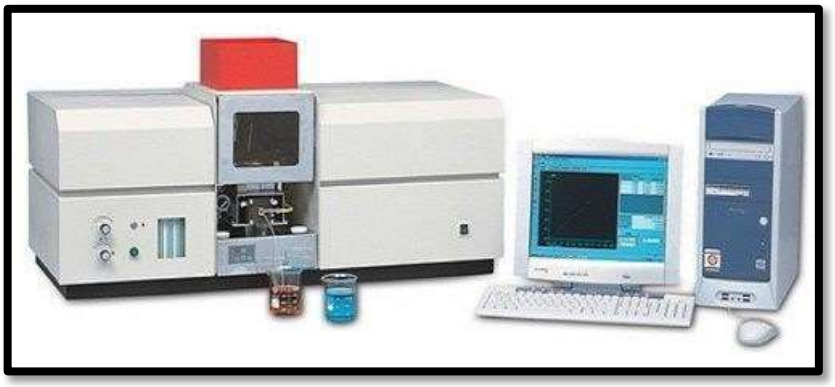

Figure (2.4): Atomic absorption spectrometry

2.6.2 X-Ray Diffraction

X-ray diffraction (XRD) is one of the most powerful techniques for qualitative analysis of crystalline compounds. In this study thin films have been examined by Bruker D2 PHASER XRD technique under the conditions power diffraction system with Cu-Kα x-ray tube (λ = 1.54056 A °). The x-ray scans are recorded with diffraction angle 2θ in the rang 20° – 60°, the overall structure of thin films, including lattice constants, gran size identification of unknown materials, orientation of single crystals and orientation of polycrystals.

The crystal structure is determined with a XRD with a Cu-Kα, radiation tube. According to Bragg s law, if the lattice planes (formed by the atoms in the crystal) are prefect and spaced by a distance d, then the reflection of a monochromatic beam takes place only at a certain angle which satisfies the following equation Bragg law [105]:

$$n\lambda = 2d\ sin\theta \text{---------- (2-1)}$$

Where λ is the wavelength of the beam and θ is the incidence angle (and the reflection angle too as reflection is assumed to the elastic). The crystallite size (C.S) can be estimated using the Scherer s equation [106]:

$$D = \frac{\lambda}{\beta\ cos\theta} \text{ ---------- (2-2)}$$

Where λ wavelength of the radiation, β full with at half maximum, θ

Bargg s diffraction angle of the peak and K= 0.94 (Scherer s constant).

2.6.3 UV- Visible

The optical absorbance spectra of the Se Colloidal are measured using UV-Visible spectrophotometer (the wavelength ranging from 350 - 1100 nm). The samples are at different concentrations and exposure time and put in a quartz cell with 1 cm optical path. The output data of wavelength, absorption are used in a computer program to deduce the absorbance spectrum, transmittance

2.6.4 Field Emission Scanning Electron Microscopy (FE- SEM)

FE-SEM determined the size and shape of the Ag NS by the drop coasting technique. The morphology of synthesized Ag NS was observed by Field Emission Scanning Electron Microscopy (FE-SEM, SIGMA VP-500, ZEISS) in Iran.

2.7 Antibacterial activity test of synthesized Nanoparticles

2.7.1 Activation and preparation of the Bacterial isolates The bacterial isolates used in this study were obtained from the Central Environmental Laboratory/College of Science/University of Baghdad; she was gram positive Bacteria (Staphylococcus. aureus) and Gram-negative bacteria (Pseudomonas. klebsiella) to assess the infection antibacterial activity of the as-prepared Nanoparticles. Lines of bacterial isolates were placed on brain heart infusion agar and incubated for 18 hours at 37°C. One colony was then picked from the media plate and inoculated in 5 ml of brain heart infusion broth and then incubated overnight at 37.°C

2.7.2 Antibacterial Activity of the Silver Nanoparticles

The antibacterial activity of selenium nanoparticles was studied using agar-well diffusion method against each of the previously mentioned microorganisms. The tested bacteria were uniformly flushed onto Muller-Hinton agar plates using a sterile cotton swab, then four 6 mm diameter wells were made using a sterile well drill. Freshly synthesized Se NPs solutions of different concentrations (6.1, 7.2, and 10) ppm were added to the corresponding wells. The samples were then incubated overnight at 37 °C. After the incubation period, the region of inhibition (in mm diameter) was observed and tabulated. After the incubation period, positive test results were recorded when an area of inhibition (in mm diameter) was observed around the well.

3.1 Introduction

This chapter includes the results of Atomic absorption, XRD diffraction; Field emission scanning electron microscope, energy Dispersive X-ray, and optical properties Characteristics of MgO colloidal Nanoparticles prepared with a pulse laser ablation and different energy. In addition, The impact of nanoparticles MgO has been studied on the bacterial activity of types of bacteria positive and negative gram.

3.2 X-Ray Diffraction

calculate for all the prepared MgO NPs by using the Nd:YAG laser with two energies (300 - 500 mJ), the crystalline size of the samples determined using the Debye-Scherrer equation (°K Debye) (3-1). Figure (3.1) shows the crystal levels for MgO NPs have face centered cubic structure appear at those at (32.56^o, 37.6^o, 43.75^o, 46.17^o, 64^o, 76.7^o) respectively, the results are agree with [100]. The average of the crystalline size for MgO NPs is increase with increasing the laser energy.

$$D = \frac{0.9\,\lambda}{\beta \cos\theta} \quad \text{..... (3.1)}$$

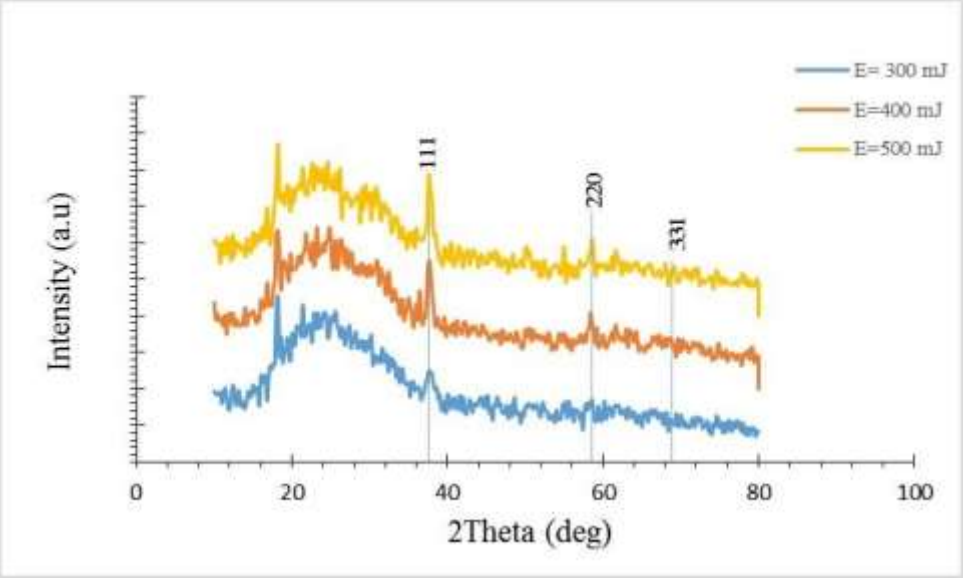

Figure (3.1): The Crystalline MgO NPs With Angle (2θ).

Table (3-1) shows the structural properties of MgO NPs.

LASER ENERGY(mJ)	FWHM	2THETA	hkl	D	Avg.
	0.15	38	111	56.14	
300	0.24	58.8	220	38.06	35.429
	0.8	69.2	331	12.08	
	FWHM	2THETA	hkl	D	Avg.
400	0.2	38	111	42.10	
	0.125	58.8	220	73.07	44.839
	0.5	69.2	331	19.32	
	FWHM	2THETA	hkl	D	Avg.
500	0.095	38	111	88.64	
	0.24	58.8	220	38.06	61.1873
	0.17	69.2	331	56.85	

3.3 Field Emission Scanning electron microscopy (FE- SEM)

FE-SEM images in 330 kx magnification powers for MgO with (300,400 and 500 mJ) but FE-SEM images in 330 kx with (300 mJ) concentrations for particular have been investigated prepared by drop costing method using scanning electron microscopy (FE-SEM) [17]., are shown in Figures(3.2). The images illustrate cubic nanoparticles crystals with different diameters for each sample aggregate with each other. The average particles size is about (100,200 and 200) nm for MgO with (300,400 and 500 mJ) for nano particle sample.

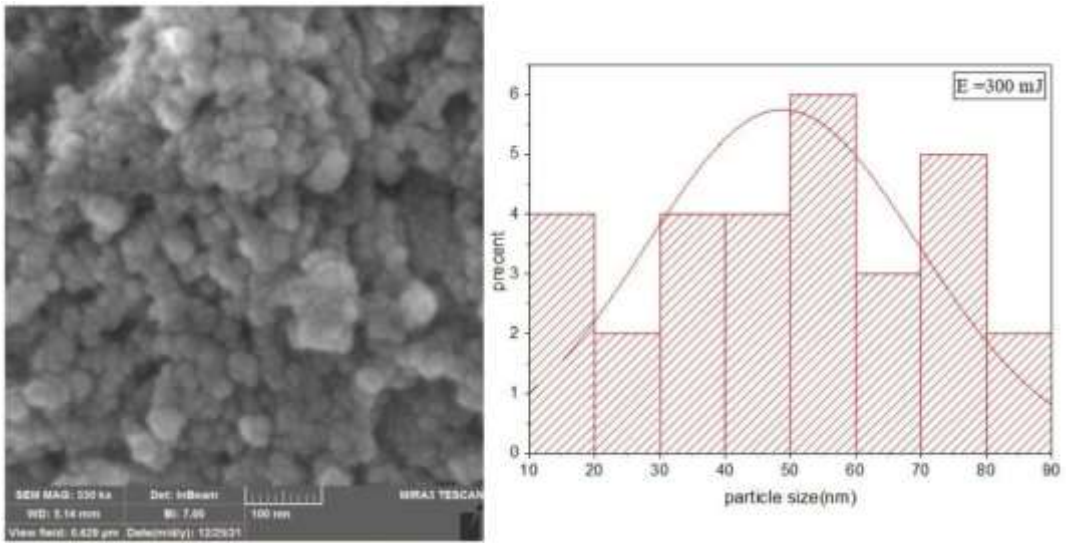

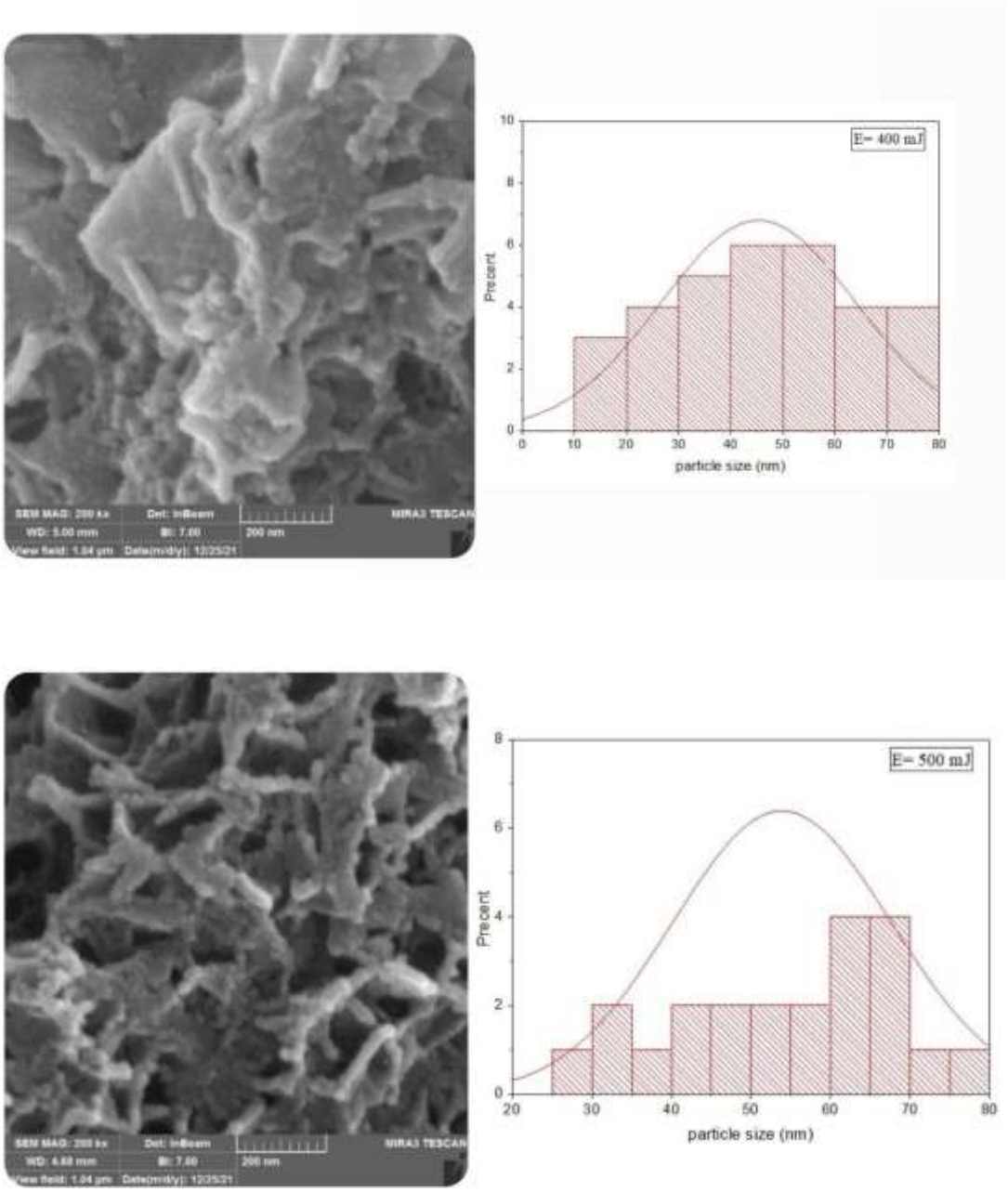

Figure (3.2). Field emission scanning electron microscopy images for of MgO nanopartical at(300,400,and 500)mJ.

3.4 Absorption Spectrum

The optical energy gap is one of the most important optical constants in semiconductor physics. The use of metal in optical and electronic applications depends on the value of this constant (Eg). The resulting spectrum obtained on MgO is shown in Figure (3.4). The spectral data

recorded showed the strong cut off at 285, 315, 337.5 nm; where the absorbance value is minimum. Figures 1 show the determination of the direct energy gap value for the MgO nanoparticle and with different concentrations of (17.4 ,27.4 and 19.4)ppm. It can be noticed that when concentrations increases, the energy gap will decreases which means the grain size decreasing. The optical energy difference was calculated by a study of the spectral dependence of absorption near the fundamental absorption. Using the Eq.(3.2) [18].

$$Eg = h*C/\lambda \ldots\ldots (3.2)$$

A decrease in the energy gap values was observed with the increase in the concentrations. This decrease can be explained by the fact that the increase in concentration led to an increase in the number of collisions of photons with the material, and therefore the material will absorb theo9 photons more, which leads to an increase in the number of electrons and holes, and thus the energy gap decreases, and this decrease leads to the regulation of the distribution of atoms Inside the material and changing crystal phases.

the energy gap will decrease which means the grain size decreasing". The explanation for this can be due to reducing extents of quantum confinement, where the large particle size (at higher concentrations) can lead to more energy states and decreased confinement effect that forms a small band gap.

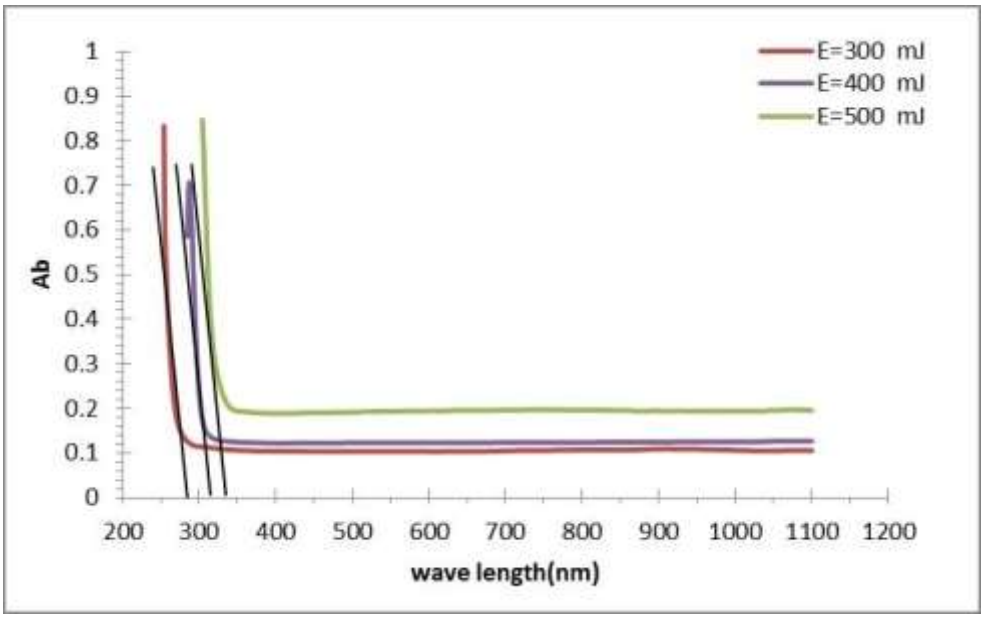

Figure (3.3). Optical Energy Gap for MgO NPs at (300,400, and 500) mJ.

Table (3.2): Calculations of energy gap of MgO NPs

Band Gap Energy (E) = h*C/λ		
h = planks constant = 6.626×10^{-34} Joules sec		
C= Speed of light =3×10^{8} meter /sec		
Laser energy (mJ)	λ= Cut off wave length (nm)	Eg(eV)
300	280	4.428571
400	310	4
500	340	3. 647058

3. 5Antibacterial Activity

The opinion of the laboratory official: The experiment was conducted under air conditions (temperature 37 °C), four types of pathogenic bacteria were developed (two Gram-negative and two Gram-positive), and all pathogenic bacterial isolates were exposed to the active compounds by etching method.

Organisms	1	2	3	control
E. coli	22 mm	25 mm	32 mm	——
Psuedomonas aeruginosa	20 mm	28 mm	32mm	——
S. aurous	——	——	——	——
Streptococcus pyogenes	——	22mm	——	——

Vehicles showed effective against one type of bacteria positive for the bacteria, a dye Almsobhah and the effectiveness of the two types of Staphylococcus bacteria large negative tinge that showed sensitivity to the effect of nanoparticles compounds and this may be attributed to the installation of a bacterial cell wall.

Refference

[1] Lehmann A, Pietag F, Arnold T. Human health risk evaluation of a microwave-driven atmospheric plasma jet as medical device. Clinical Plasma Medicine. 2017;7:16-23.

[2] Chen FF. Introduction to plasma physics and controlled fusion: Springer; 1984.

[3] Nehra V, Kumar A, Dwivedi H. Atmospheric non-thermal plasma sources. International Journal of Engineering. 2008;2(1):53-68.

[4]]Amudha Murugan, Krishna Kumara, shanmugasundaram, "Biosynthesis and characterization of silver nanoparticles using the aqueous extract of vitex negundo", World Journal of Pharmaceutical Sciences, vol. **3(8)**, (2014): 1385-1393

[5] Siavash I ravani, Behzad Zolfaghari, "Green synthesis of silver nanoparticles using Pinus eldarica bark extract". BioMed Research Internatinal, volume (2013).

[6] Sonali Pradhan, " Comparative analysis of Silver Nanoparticles prepared form Different Plant extracts (Hibissus rosa sinensis, Moringaolifera, Acorus calamus, Cucurbita maxima, Azadirachat indica) through green synthesis method", MSc thesis. National Institute of Techonology, Rourkela, (2013) pp:73.

[7] Jitendra Mittal, Amla Batra, Amla Batra, Abhijeet Singh and Madan Mohan Sharma, "Phytofabrication of nanofactories through plant as nanofactories" Advance in Natural Sciences: Nanoscience and Nanotechnology , vol.**5** (2014), pp:10.

[8] Varahalarao Vadlapudi, Kaladhar, D.S.V.G.K., Mohan Behara, Sujatha, B., Kishore Naidu, G. "Synthesis of green metallic nanoparticles (NPs) and application". Oriental Journal of Chemistry,

vol. **29(4)** (2013): 1589-1595.

[9] Jonathan L., Juan. P,D.K.Y. Low and Ehsan. T,"ADVANCES IN LASER PROCESSING OF MATERIALS", Published in Association with EMRS, (2006):pp848

[10] M. Kim, S. Osone, T. Kim, H. Higashi, and T. Seto, "Synthesis of Nanoparticles by Laser Ablation: A Review" KONA Powder and Particle Journal, vol. **10**, no.34 (2016):80–90.

[11] A. Singh, J. Vihinen, E. Frankberg, L. Hyvärinen, M. Honkanen and E. Levänen, , "Pulsed Laser Ablation-Induced Green Synthesis of TiO2 Nanoparticles and Application of Novel Small Angle XRay Scattering Technique for Nanoparticle Size and Size Distribution Analysis," Nanoscale Res. Lett., vol. **11**, no. 1 (2016) 1–9.

[12] P. V. Kazakevich, A. V. Simakin, V. V. Voronov, and G. A. Shafeev, "Laser induced synthesis of nanoparticles in liquids" , Applied Surface Science, vol. **252**, no.13 (2006) 4373–4380.

[13] J. Xiao, P. Liu, C. X. Wang, and G. W. Yang, "External field assisted laser ablation in liquid: An efficient strategy for nano crystal synthesis and nanostructure assembly," Progress in Materials Science, vol. **87**, no. 2 (2017) 140–220.

[14] A. M. Darwish, W. H. Eisa, A. A. Shabaka, and M. H. Talaat, "Investigation of Factors Affecting the synthesis of nano-cadmium sulfide by pulsed laser ablation in liquid Environment", Spectrochimica Acta Part A Molecular Biomolecular Spectroscopy, vol.**153** (2016):315-320

[15] V. Amendola and M. Meneghetti, "What controls the composition and the structure of nanomaterials generated by laser ablation in liquid solution", Physical Chemistry, vol. **15**, no. 9 (2013) 3027–3046.

[16] J. Zhang, J. Claverie, M. Chaker, and D. Ma, "Colloidal Metal Nanoparticles Prepared by Laser Ablation and their Applications,"

Physical Chemistry, vol. **18** no. 9 (2017):986–1006.

[17] Eliezer S, Eliezer Y. The fourth state of matter: an introduction to plasma science: CRC Press; 2001.

[18] Fridman A. Plasma chemistry: Cambridge university press; 2008.

[19] Ercan UK, Wang H, Ji H, Fridman G, Brooks AD, Joshi SG. Nonequilibrium Plasma-activated antimicrobial solutions are broad-spectrum and retain their efficacies for extended period of time. Plasma processes and polymers. 2013;10(6):544-55.

[20] Nemukhin A. MI Boulos, P. Fauchais, and E. Pfender," Thermal Plasmas: Fundamentals and Applications", New York: Plenum, 1994, vol. 1. RUSSIAN JOURNAL OF PHYSICAL CHEMISTRY C/C OF ZHURNAL FIZICHESKOI KHIMII. 1996;70:177-.

[21] Heberlein J. New approaches in thermal plasma technology. Pure and applied chemistry. 2002;74(3):327-35.

[22] Ginsberg G, Barkun A, Bosco J, Burdick J, Isenberg G, Nakao

N. Technology status evaluation report: The argon plasma coagulator. Gastrointest Endosc. 2002;55(7):807-10.

[23] E.A. Coronado, E. R. Encinaa and F. D. Stefan," Optical properties of metallic nanoparticles: manipulating light, heat and forces at the nanoscale" Nanoscale, 3(10), 2011.

[24] Collee , J.G.; fraser , A.G.; Marmion ,B.P.and Simmons

,A.Mackie and McCartney,"practical Medical Microbiology",14th editi Churchil living stone,New York,(1996)

[25] Farfan, M.J.; Torres, A.G." Molecular mechanisms that mediate colonization of Shiga toxin-producing Escherichia coli strains",Infect Immune . 80(3):903-913,(2012).

[26] Balcht ،Aldona; Smith ،Raymond (1994). Pseudomonas aeruginosa: Infections and Treatment. Informa Health Care. Pp.

83–84. ISBN 0-8247-9210-6.

[27] Wexler DE, Chenoweth DE, Cleary PP (1985) ،"Mechanism of action of the group A streptococcal C5a inactivator" ،Proc Natl Acad Sci USA ،82 (23): 8144–8 ،doi:10.1073/pnas.82.23.8144 ،

PMC 391459 ،PMID 39

[28] "Streptococcus pyogenes NZ131" ،11 May 2020.

[29] Ferretti JJ ؛McShan WM ؛Ajdic D ؛Savic DJ ؛Savic G ؛Lyon K ؛ " ،)2001(Complete Genome Sequence of an M1 Strain of Streptococcus pyogenes" ،Proc Natl Acad Sci USA ،98: 4658–

63 ،doi:10.1073/pnas.071559398 ،PMC 31890 ،PMID

11296296.